Deformation and signature splitting in ^{74}Br

J.W. Holcomb, T.D. Johnson, P.C. Womble, P.D. Cottle, and S.L. Tabor
Department of Physics, Florida State University, Tallahassee, Florida 32306

F.E. Durham and S.G. Buccino
Department of Physics, Tulane University, New Orleans, Louisiana 70118
(Received 20 July 1990)

The high-spin states of ^{74}Br were studied via the ^{48}Ti(^{32}S,αpn)^{74}Br and the ^{58}Ni(^{19}F,$2pn$)^{74}Br fusion-evaporation reactions at energies of 105 and 62 MeV, respectively, using the Florida State University Tandem LINAC. γ-γ coincidence arrays were produced using four Compton-suppressed Ge detectors. Two independent groups of γ rays were studied — one of positive parity and one of negative parity, both of which appear to be based on an isomeric $4^{(+)}$ state. Lifetimes were measured using both the Doppler-shift attenuation and recoil-distance methods. A cranking-model analysis of the bands shows that the kinematic and dynamic moments of inertia for the bands are rather similar and fairly constant for high spins with values of (20–23)$\hbar^2$/MeV. A phase reversal occurs in the signature splitting in the yrast band around spin 9 which is related to the quasiparticle alignments. The lifetimes imply an average axial quadrupole deformation of 0.37 in the yrast band and 0.34 in the negative-parity band. These deformations are close to those predicted by Hartree-Fock-Bogolyubov cranking calculations.

I. INTRODUCTION

Nuclei in the *f-p-g* shell illustrate rather well the interplay between single-particle and collective degrees of freedom. Highly collective behavior with rotational bands exhibiting quadrupole deformations exceeding 0.4 is not uncommon near the middle of the shell, yet nearly spherical shapes coexist at similar energies in some nuclei. An odd nucleon can polarize the core to quite different shapes depending on the orbital occupied, as was demonstrated[1,2] in ^{81}Sr. The alignment of a pair of quasiparticles can further affect the deformation, often to triaxial shapes.

The shape driving effects of the two quasiparticles in odd-odd nuclei have not been investigated as thoroughly. A number of other effects might also be expected from the unpaired nucleons. Each odd $g_{9/2}$ particle can contribute considerable intrinsic spin to the system, and each will block the lowest band crossing through the Pauli principle. Members of the $\pi g_{9/2} \otimes \nu g_{9/2}$ multiplet can also mix with lower spin rotational states.

Good rotational bands can often be seen in these odd-odd nuclei but the energies of the low-spin states tend to deviate from what is expected for a rigid rotor. The change occurs[3] around spin $8\hbar$ in ^{78}Rb and Kreiner and Mariscotti predicted[4] a change in ^{76}Br near $9\hbar$ from a two-quasiparticle-plus-rotor calculation. In their calculation the change shows up most clearly as a phase inversion in the signature splitting. Below $9\hbar$ both rotation and realignment of the intrinsic spins contribute to the total angular momentum, while additional angular momentum above this point comes only from rotation. García Bermúdez *et al.* saw[5] a similar phase change in ^{74}Br but the ^{76}Br level scheme was not known above the point of expected change at that time.

The present investigation of ^{74}Br and a companion study[6] of ^{76}Br were undertaken to address some of these questions in the odd-odd Br isotopes. Previously, García Bermúdez *et al.*[5] had investigated the yrast band of ^{74}Br up to a probable spin of $11\hbar$ and two other decay sequences to lower spins. Winter *et al.*[7] reported 4 bands or decay sequences populated in light-ion-induced reactions. The yrast band was observed up to $10\hbar$. In a conference proceedings Neumann *et al.*[8] showed the level scheme for two bands in ^{74}Br, including one state above the spin (12) member of the yrast band. Neumann *et al.* also listed the only lifetimes which have been reported in ^{74}Br, a set of 8 values measured with the recoil-distance method. Most of the lifetimes imply collective electric quadrupole transition strengths [$B(E2)$] of 50 to 100 single-particle units (W.u.), which are typical of the well-deformed nuclei in this region. However, a lifetime of 73.3±4.0 ps was reported for the $(11) \rightarrow (9^+)$ transition, which gives a $B(E2)$ value of 0.74 ± 0.11 W.u. A band crossing at this frequency (as the anomalously low transition strength was interpreted) would be very interesting.

An additional complication in the odd-odd ^{74}Br is the existence of a spin-4 isomer 100–200 keV above the spin (0,1) ground state. Some uncertainties remain about the parities of these states and about which one the various bands decay into. The available evidence is summarized

in Sec. III A.

In the present work high-spin states in ^{74}Br were populated in two heavy-ion fusion-evaporation reactions. Two rotational bands were extended up in spin to study the rotational behavior well above the change in signature splitting around spin 9. Lifetimes were measured using the Doppler-shift attenuation and recoil-distance methods to study the transition strengths and deformations and to investigate the anomalously low $B(E2)$ value. The deformations were compared with the predictions of Hartree-Fock-Bogolyubov cranking calculations.[9]

II. EXPERIMENTAL TECHNIQUES

The techniques of γ spectroscopy were applied to investigate the high-spin states of ^{74}Br. The results presented here are based on experiments using two different reactions. In the first, ^{74}Br was populated using the ^{48}Ti(^{32}S,αpn) reaction with a 106 MeV ^{32}S beam from the Florida State University Tandem LINAC facility incident on a 0.5-g/cm^2 natural Ti target. A 62 MeV ^{19}F beam from the tandem accelerator alone on a 19-mg/cm^2 enriched ^{58}Ni foil was used for the ^{58}Ni(^{19}F,$2pn$)^{74}Br reaction.

In the first reaction, four 25% efficient high-purity Ge γ detectors placed in bismuth germanate (BGO) Compton-suppression shields were used to measure the γ-γ coincidences from the reaction. Three detectors were placed at 95° while the fourth was placed at an 18° angle with respect to the beam. The forward angle was chosen to allow measurements of lifetimes of the high-spin states via the Doppler-shift attenuation method. In the ^{19}F experiment, two Compton-suppressed Ge detectors were placed at 90° with a third at 4° with respect to the beam axis. A fourth detector without Compton suppression was placed at 140° to facilitate the recoil-distance measurements. More than 6 × 10^8 γ-γ coincidences were recorded on magnetic tape for each experiment. Internal energy calibrations for the sulfur reaction were made using a least-squares fitting of energies of the following gamma rays (in keV) to a linear function of channel number: 179.1 and 300.2 (^{77}Kr), 423.9 (^{76}Kr), 634.8 (^{74}Se), 983.5 (^{48}Ti), 1227.7, and 1524.6 (^{42}Ca). An excellent fit was obtained for the linear regression of the corresponding energies and channel numbers. The events between any two of the three 95° detectors were then gainshifted to a dispersion of 0.8 keV/channel and sorted[10] into a 2500 channel triangular array on a RIDGE3200 computer. The events between the 18° detector and any of the 95° ones were gainshifted and sorted into a 2500 × 2500 channel square array. Internal energy calibrations for the fluorine reaction were made using a least-squares fitting of energies (in keV) of the following gamma rays: 74.9 (Pb x ray), 188.4 (^{74}Br), 197.15 (^{19}F), 511.0 (γ^{+-}), 634.8 (^{74}Se), and 1000.2 (^{71}As). These events were sorted and histogrammed into four two-dimensional arrays corresponding to the four detector angle pairs.

III. THE LEVEL SCHEME

The present level scheme was deduced from coincidence spectra generated from gating on the two-dimensional arrays. Placement of the transitions in the level scheme was determined from the 90° spectra. To determine the multipolarities of the transitions, directional correlation of oriented nuclei (DCO) ratios were calculated wherever possible. The DCO ratios ($R_{\rm DCO}$) were determined from gating on the square matrix and comparing the intensities according to

$$R_{\rm DCO} = \frac{I(\gamma \text{ at } 18° \text{ gated by } \gamma_G \text{ at } 95°)}{I(\gamma \text{ at } 95° \text{ gated by } \gamma_G \text{ at } 18°)} , \quad (1)$$

where the coincidence gate was always from one or more of the $E2$ transitions. Unmixed $E2$ transitions are expected to yield a DCO ratio of approximately 1, while, depending on the multipole mixing ratio, the DCO ratio of a $\Delta J = 1$ transition can vary from 0 to 2. It is expected, however, that most $M1/E2$ DCO ratios in the yrast and near-yrast cascades will be near $\frac{1}{2}$.[2,11] Energies, intensities, and DCO ratios for the transitions are listed in Table I. The energies reported are those determined in the present work, but generally agree with previous results.

A. Spin and parity of the bandhead

Studies of the β decay of ^{74}Kr (Refs. 12–14) and ^{74}Br (Ref. 15) established two long-lived β decaying states in ^{74}Br. Only the low-spin state (0^- or 1^-) with a half-life of 25.7 min is populated in the β decay of ^{74}Kr. Both this state and a higher-spin state ($J = 4$) with a half-life of 41.5 min (Ref. 15) or 49.5 min (Ref. 5) have been populated directly in nuclear reactions. A possible reason for the difference in half-lives is discussed in Ref. 5. The present work provides no new information concerning the lifetime of the isomer, nor are the conclusions of this report sensitive to its exact value. The newer value, 49.5 min, is used in this report mainly as a label for the state. The level ordering was determined in a ^{74}Se(p,n)^{74}Br excitation function measurement[16] which established that the 25.7 min low-spin state is the ground state and the 49.5 min spin-4 isomeric state lies 135 to 255 keV higher in energy.

An unambiguous spin assignment of $4\hbar$ was determined for the 49.5 min isomeric state in an atomic-beam magnetic-resonance experiment.[17] There was no evidence for population of the 25.7 min ground state in the spallation reaction used for that experiment. Although the spin of the isomeric state is well established, questions remain about its parity. An assignment of J^π=4$^-$ was made[15] based on the β decay of ^{74}B^m to states in ^{74}Se. Although negative parity is consistent with the large logft values observed for decays to 2^+ and 4^+ states, positive parity is not ruled out, as has been emphasized by Raman and Gove.[18] For example, Winter *et al.*[7] have suggested that the β decay may be hindered by K forbiddeness,

rather than a parity change. The fact that the γ-decay sequence built on this isomer in ^{74}Br more closely resembles that built on the 4^+ state[19] in the neighboring ^{76}Br than that built on the 4^- state in ^{76}Br led Winter *et al.* to propose $J^\pi=4^+$ for the ^{74}Br^m state. The present work and a companion study[6] of ^{76}Br show that the ^{74}Br-^{76}Br resemblance continues to the highest spins observed. Therefore a positive sign in parentheses will be used to indicate that positive parity is likely, but not fully proved, for the 49.5 min isomeric state in ^{74}Br.

B. The yrast band

García Bermúdez *et al.*[5] found that the spin-4 isomer was populated much more strongly than the ground state in the ^{60}Ni(^{16}O,$np\gamma$) reaction and identified the most intense γ-decay sequence (188.5, 195.0,... keV) with the spin-4 state. Winter *et al.*[7] made the same assignment using the relative populations of states in d and ^{3}He induced fusion-evaporation reactions as a "spin meter." The 188.5, 195.0,... keV decay sequence is also the most

TABLE I. Energies, relative intensities, DCO ratios, and multipolarities for transitions in ^{74}Br.

				R_{DCO}		
E_{lev} (keV)	E_γ (keV)	$I_i \rightarrow I_f$	Int.	S+Ti	F+Ni	ΔJ
188.5	188.5	$5^{(+)} \rightarrow 4^{(+)}$	89	0.20(2)	0.22(1)	1
383.4	383.4	$6^{(+)} \rightarrow 4^{(+)}$	44	0.89(8)	0.95(3)	2
	195.0	$6^{(+)} \rightarrow 5^{(+)}$	56	0.21(2)	0.26(2)	1
656.1	467.5	$7^{(+)} \rightarrow 5^{(+)}$	11			2
	272.8	$7^{(+)} \rightarrow 6^{(+)}$	21	0.29(2)	0.23(3)	1
812.5	429.2	$8^{(+)} \rightarrow 6^{(+)}$	39	1.07(8)	0.97(7)	2
	156.4	$8^{(+)} \rightarrow 7^{(+)}$	8.2	0.34(5)	0.53(8)	1
1160.2	504.1	$9^{(+)} \rightarrow 7^{(+)}$	3.3			2
	347.8	$9^{(+)} \rightarrow 8^{(+)}$	19	0.34(2)	0.32(2)	1
1646.5	833.9	$10^{(+)} \rightarrow 8^{(+)}$	22	1.11(21)	0.98(8)	2
	486.3	$10^{(+)} \rightarrow 9^{(+)}$	1.4			1
2054.3	894.1	$11^{(+)} \rightarrow 9^{(+)}$	8.0		0.94(12)	2
	407.8	$11^{(+)} \rightarrow 10^{(+)}$	7.0	0.32(10)	0.33(3)	1
2752.2	1105.7	$12^{(+)} \rightarrow 10^{(+)}$	6.7	1.09(20)	1.04(9)	2
	697.9	$12^{(+)} \rightarrow 11^{(+)}$	2.0			1
3163.2	1108.9	$13^{(+)} \rightarrow 11^{(+)}$	11	1.09(20)	1.04(9)	2
4083.4	1331.2	$(14^+) \rightarrow 12^{(+)}$	4.8			2
4478.7	1315.5	$(15^+) \rightarrow 13^{(+)}$	5.2			2
5600.8	1517.4	$(16^+) \rightarrow (14^+)$	2.7			2
5948.7	1470.0	$(17^+) \rightarrow (15^+)$	3.2			2
7600.9	1652.2	$(19^+) \rightarrow (17^+)$	1.7			2
72.1	72.1	$(3^-) \rightarrow 4^{(+)}$				1
188.4	188.4	$(4^-) \rightarrow 4^{(+)}$	15		0.46(20)	1
	116.2	$(4^-) \rightarrow (3^-)$	38	0.34(7)	0.35(3)	1
357.7	285.9	$(5^-) \rightarrow (3^-)$	7.5	1.02(19)	1.07(13)	2
	169.3	$(5^-) \rightarrow (4^-)$	13	0.36(4)	0.31(4)	1
606.4	418.0	$(6^-) \rightarrow (4^-)$	6.1	0.92(6)	0.67(11)	2
	248.7	$(6^-) \rightarrow (5^-)$	3.3			1
848.2	490.4	$(7^-) \rightarrow (5^-)$	6.3	0.97(26)	1.07(14)	2
	241.8	$(7^-) \rightarrow (6^-)$	2.3	0.64(27)	0.38(6)	1
1259.5	653.0	$(8^-) \rightarrow (6^-)$	1.9	0.97(22)	1.11(22)	2
	411.3	$(8^-) \rightarrow (7^-)$	2.1		0.25(5)	1
1674.4	826.2	$(9^-) \rightarrow (7^-)$	4.9	0.93(15)	0.85(13)	2
	415.1	$(9^-) \rightarrow (8^-)$	0.5			1
2126.9	867.4	$(10^-) \rightarrow (8^-)$	3.4	0.98(22)	1.03(8)	2
	452.3	$(10^-) \rightarrow (9^-)$	0.9			1
2602.5	928.1	$(11^-) \rightarrow (9^-)$	3.4		0.96(28)	2
	475.9	$(11^-) \rightarrow (10^-)$	0.4			1
3142.8	1015.9	$(12^-) \rightarrow (10^-)$	4.1			2
3670.6	1068.1	$(13^-) \rightarrow (11^-)$	3.1			2
4327.7	1184.9	$(14^-) \rightarrow (12^-)$	2.2			2
4895.0	1224.4	$(15^-) \rightarrow (13^-)$	1.2			2

intense in the present ^{19}F-induced reaction and, therefore, must be yrast and built on the higher-spin isomer. The level scheme in Fig. 1 shows this placement. Note that all level energies are shown relative to the isomer, which itself lies 135 to 255 keV above the ground state.

The previously deduced level scheme for the yrast band[5,7,8] was generally confirmed and extended by the present work up to a spin of (19^+).

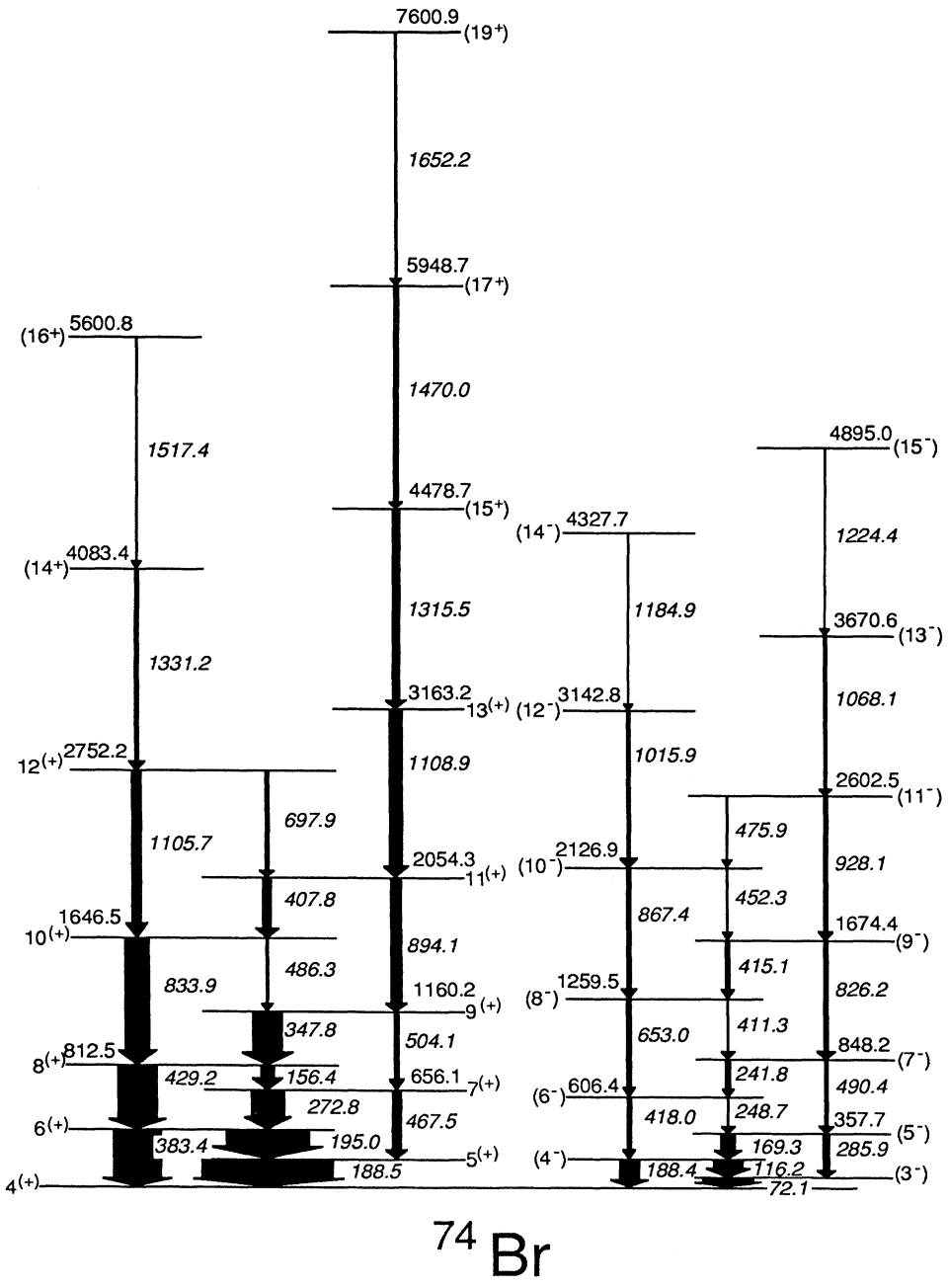

FIG. 1. The high-spin level scheme of ^{74}Br deduced from the present and previous work. Only the yrast and yrare bands are shown. Note that the excitation energies are given relative to the 4^+ isomer whose exact position relative to the ground state is unknown. The bandhead spins, parities, and placements are discussed in the text, and some uncertainties remain, especially for the (3^-) band.

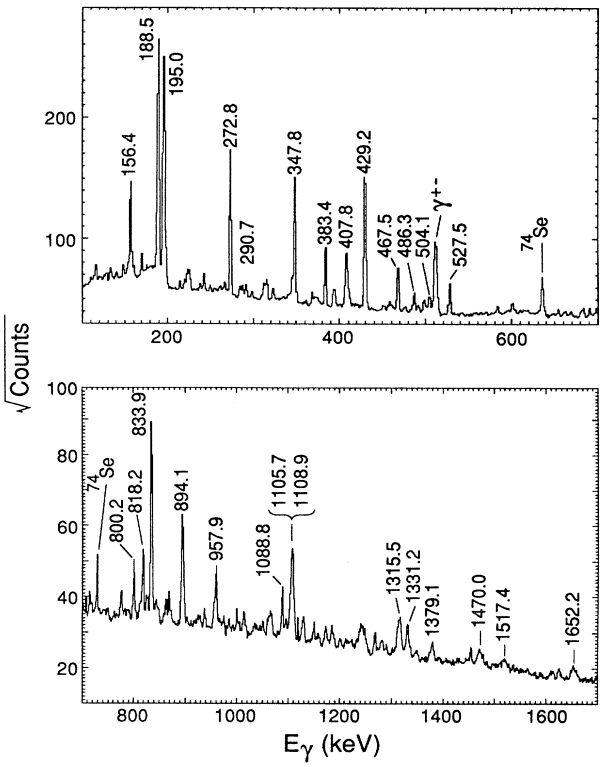

FIG. 2. The spectrum of γ rays from the ^{58}Ni(^{19}F,2pn)^{74}Br reaction in coincidence with any of the strong lines in the yrast band. The square root of the number of counts is graphed to provide a moderate compression of the dynamic range.

Shown in Fig. 2 is a sum spectrum of gates on yrast lines from the ^{58}Ni(^{19}F,2pn) reaction. In addition to the transitions between yrast states, some side-feeding transitions (which will be discussed later) are also easily observed. The transitions with DCO ratios consistently near unity, i.e., values ranging from 0.89 to 1.11, were assigned to have $\Delta J = 2$. Transitions with DCO ratios ranging from 0.20 to 0.53 were assigned to have $\Delta J = 1$. Due to lack of statistics or difficulty in determining the total yield in the forward spectra, ratios could not be determined for the following transitions: 467.5, 504.1, 486.3, 697.9, 1315.5, 1331.2, 1470.0, 1517.4, and 1652.2 keV. Tentative spin assignments for the 14^+ to 19^+ states were proposed based on the systematic behavior of rotational bands.

C. The negative-parity band

There is less agreement in the literature regarding the placement of the γ-decay cascade ending in the 72.1 keV transition. García Bermúdez *et al.*[5] placed it on a low-spin $(0,1^-)$ state at low energy ($E_x < 30$ keV) based on excitation curves, although intensity arguments did not rule out its placement on the 4^+ isomer. Neumann *et al.*[8] placed it on the ground state whose spin is also $(0,1^-)$. Winter *et al.*[7] placed the sequence on the 4^+ isomer based on the relative intensities in the d- and ^{3}He-induced reactions and on their excitation curves. They found further evidence from the pattern of β decay to ^{74}Se which indicated that most prompt γ rays lead to population of the isomer. We have also placed the 72.1 keV decay sequence atop the 4^+ isomer because its strong population in these heavy-ion reactions argues strongly for higher spin. By contrast, we see almost no population of the 62.8, 128.3,... keV decay sequence which previous work[5,7] has consistently placed on the low-spin ground state.

It should be emphasized that there is no hard evidence concerning the spin, parity, or placement of the bandhead for this cascade. This is the reason for the variation in the literature. Our assignment appears the most likely based on all the indirect evidence and is not inconsistent with the evidence. For example, the 72.1 and 188.4 keV transitions to the isomer would have $E1$ strengths of 7×10^{-5} and 2×10^{-5} Weisskopf units (W.u.) based on the indicated spins and the lifetimes of Ref. 7. These are similar to other known values in this mass region. Similarly the 116.2 keV transition would have a reasonable $M1$ strength of 0.015 W.u.

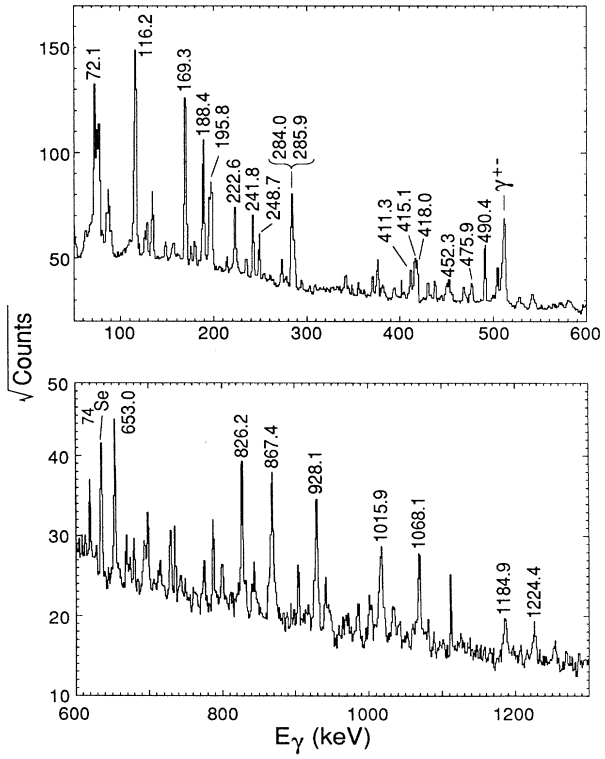

FIG. 3. The spectrum of γ rays from the ^{58}Ni(^{19}F,2pn)^{74}Br reaction in coincidence with any of the strong lines in the negative-parity band.

Negative parity has generally been suggested[5,7] for this band but the evidence is not conclusive. Since our placement of the band is similar to that of Winter *et al.*, we have followed their spin suggestions. The spins and parities of all states in this band have been placed in parentheses because of the uncertainty of the bandhead spin parity. However, the relative spins and parities are determined as well as in any other rotational band.

This presumably negative-parity band (NPB) has been extended to a tentative spin of 15^- with observed $\Delta J = 1$ transitions up to spin 11^-. In Fig. 3, a sum 90° spectrum of the gates on the dominant lines from the ^{58}Ni(^{19}F,2*pn*) reaction is shown for this band. Seven previously unseen transitions have been added by the present work. As expected, two main $\Delta J = 2$ cascades have been observed with interconnecting $\Delta J = 1$ transitions, some of which can be seen in Fig. 4, up to spin 11.

The level scheme deduced from present coincidence spectra generally agrees with previous work.[5,7,8] There are, however, a few differences with Neumann *et al.*[8] in addition to the placement of the band. Five previously reported transitions which built a third cascade were not seen. Also, Fig. 4 shows the 90° spectrum in coincidence with the 490.4 keV transition. Clearly, the 418.0 keV transition is not in coincidence with the 490.4 keV transition.

Once again, DCO ratios were used to determine the multipolarity of the transitions. Transitions with DCO ratios varying from 0.85 to 1.11 were assigned $\Delta J = 2$ while those with ratios of 0.25 to 0.64 were assigned $\Delta J = 1$. No DCO ratios could be determined for the 248.7, 475.9, 1015.9, 1068.1, 1184.9, and 1224.4 keV transitions because of lack of statistics or difficulty in determining the total yield in the forward spectrum. Due to the presence of the 74.9-keV Pb x ray, a reliable DCO ratio could not be determined for the 72.1 keV transition. Cascade placement for the high-energy transitions was determined from the coincidence spectra. Tentative spins were assigned according to rotational systematics where DCO ratios could not be determined.

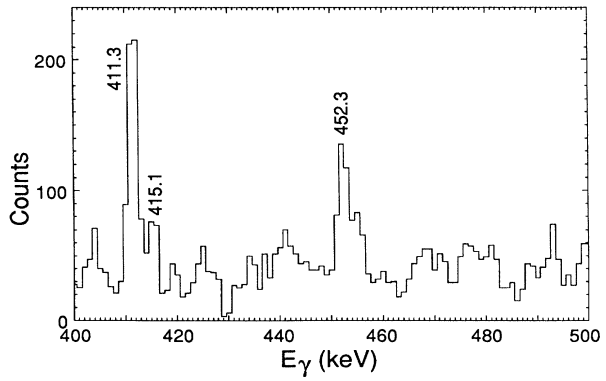

FIG. 4. A portion of the γ spectrum in coincidence with the 490.4 keV transition showing the absence of a 418.0 keV line. The peaks indicated represent $\Delta J = 1$ transitions in the negative-parity band.

D. Other transitions

In addition to the transitions shown in Fig. 1, previously reported and unreported transitions were observed in the present work. In the positive-parity band (PPB), the 527.5, 290.7, 818.2, 800.2, 957.9, and 1088.8 keV transitions of Ref. 8 were all observed in both reactions. Present coincidence spectra also support the previous placement of these transitions. Also, a 1379.1 keV transition is believed to directly feed the parent state of the 957.9 keV transition. This placement is deduced from both reactions in the present work. In the NPB, the 222.6, 284.0, and 195.8 keV lines of Ref. 8 were observed in both reactions with no disagreement in the placement.

IV. LIFETIME MEASUREMENTS

Previous work included lifetime measurements using the recoil-distance method (RDM).[8] Because of restrictions of the RDM, short-lived states could not be measured. These shorter lifetimes can, however, be measured using the Doppler-shift attenuation method (DSAM).

A. Doppler-shift attenuation

A computer code[2] that simulates the recoil slowing down process was used to extract lifetimes for the higher-spin states via DSAM. The code generates a theoretical line shape for each lifetime, using scaled stopping powers from Northcliff and Schilling,[20] and compares it to the measured forward spectrum. The value taken is the lifetime which most closely reproduces the experimental results. Uncertainty in the lifetime is determined by the rate of variation in the accuracy of the fit with the lifetime values themselves. Lifetimes for the highest measurable state for each cascade were extracted first, followed by those for each lower state. The lifetimes measured for states above each shifted line were used to specify the direct feeding times for the state. A side-feeding time of 0.05 ps was used for the (15^+) state in fitting the 1315.5 keV shifted peak. Side-feeding times were increased by approximately 0.03 ps for every MeV deexcitation energy down the cascade. Examples of best fits from the present work can be seen in Fig. 5.

For the yrast states, lifetimes for the 10^+ through the 15^+ states were determined. A mean life of 1.19 $\pm$ 0.14 ps was determined for the 10^+ state which is in agreement within uncertainty of Neumann's 1.5 $\pm$ 0.5 ps measurement.[8] For the spin-11^+ state, however, fits of the 894.1 keV peak from both reactions differ greatly from the previously reported lifetime[8] of 73.3 $\pm$ 4 ps. With an observed Doppler shift, it can be concluded that the lifetime of the 11^+ state cannot be of that order of magnitude. A lifetime of 73.3 ps would

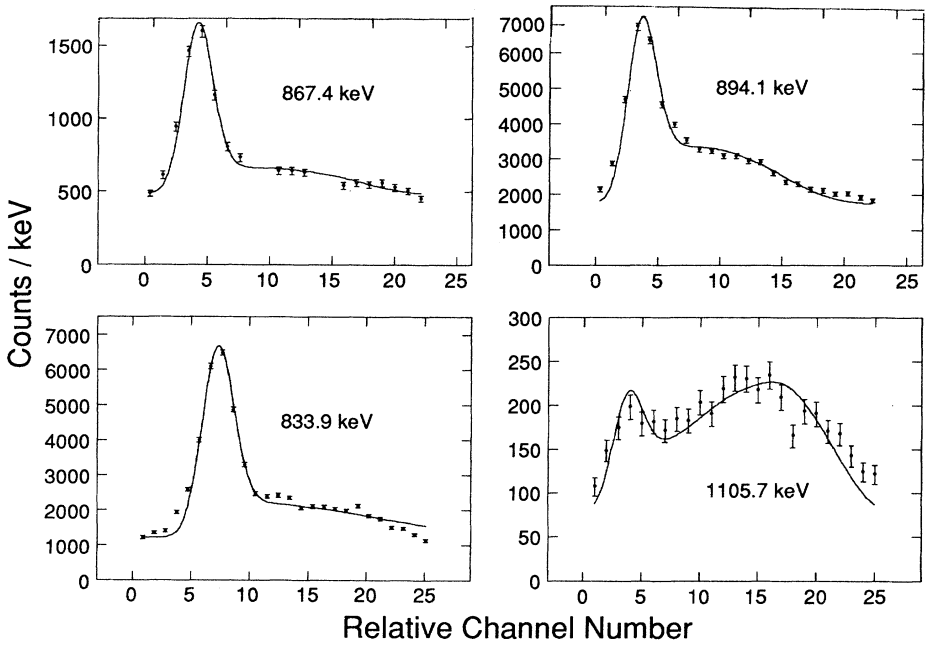

FIG. 5. Examples of forward-angle coincidence line shapes and the best-fit Doppler-shift attenuation simulations.

imply a quadrupole transition strength of 0.7 single-particle units, which is inconsistent with collective rotation. Therefore, the present value of 0.45 ± 0.15 ps was adopted and used in later analyses.

Because of the inability to correct for feeding in the highest transition of each cascade, the mean life determined in these cases serves as an upper limit to the true mean lifetime. The lifetimes corresponding to the best-

TABLE II. Shown are the lifetimes from the different reactions. Accepted values are in the final column.

I^π	τ (ps)[a]	τ (ps)[b]	τ (ps)[c]	τ_{acc} (ps)
		Recoil distance		
$5^{(+)}$			165(30)	165(30)
$6^{(+)}$	68(8)		46(10)	68(8)
$7^{(+)}$	15(1)		13(2)	13(2)
$8^{(+)}$	19(1)		23(7)	23(7)
(7^-)	17(1)			17(1)
		Doppler-shift attenuation		
$10^{(+)}$	1.5(5)	1.17(12)	1.21(15)	1.19(14)
$11^{(+)}$	73.3(40)	0.66(25)	0.35(9)	0.45(15)
$12^{(+)}$		<0.31	0.23(6)	0.23(6)
$13^{(+)}$		<0.31	0.21(5)	0.21(5)
(14^+)			<0.19	<0.19
(15^+)			<0.24	<0.24
(9^-)		0.60(20)		0.60(20)
(10^-)		0.85(14)	0.55(20)	0.70(17)
(11^-)		0.63(15)	0.46(10)	0.54(12)
(12^-)		<0.50	<0.65	<0.50
(13^-)		<0.53	<0.67	<0.53

[a] From Ref. 8.
[b] From ^{48}Ti(^{32}S,αpn).
[c] From ^{58}Ni(^{19}F,$2pn$).

fit curves are presented in Table II with adopted values in the last column.

Lifetimes for five negative-parity states were also extracted using DSAM. Once again, the lifetime for the highest state in each cascade serves as an upper bound value. These can also be seen in Table II.

B. Recoil distance

As part of the ^{58}Ni(^{19}F,2pn)^{74}Br study, approximately 10^8 coincidences were recorded using a thin target to provide recoil-distance measurements (RDM) of longer lifetimes. Drift distances of 0.25 mm and 0.64 mm to the catcher foil were used to allow a wide range of lifetimes to be measured. From a measurement of the Doppler shifts of the peaks, a consistent drift velocity of 0.0172c was determined. Drift times were, therefore, 49 and 123 ps, respectively.

Lifetimes for the $5^{(+)}$ to $8^{(+)}$ states were measured. A small unshifted peak was observed for the 347.8 keV peak with less than 10% of the total yield (shifted plus unshifted peaks), while no unshifted peaks were seen above the $9^{(+)}$ level. This implies a lifetime upper limit of 21 ps for the $9^{(+)}$ state. From the 195.0 keV gate shown in Fig. 6, a lifetime of 23 ps was deduced for the $8^{(+)}$ state with 23% and 20% of the total yield comprising the stopped peak in the 4° and 140° spectra, respectively. From the 188.5 keV gate, a lifetime of 13 ps is implied from the 23% stopped peak yield of the 272.8 keV transition. A lifetime of 46 ps was determined for the $6^{(+)}$ state from spectra gated on the 429.2 keV peak. Because of difficulty in eliminating effects of the Coulomb excitation peak of fluorine which forms a doublet with the 195.0 keV peak, this lifetime is questionable; therefore, the previously reported lifetime[8] was taken as the adopted value. Using an effective lifetime of 96 ps for the $6^{(+)}$ state, a lifetime of 172 ps was extracted from the peaks in the 4° and 140° spectra in coincidence with the 194.9 keV gate. RDM lifetimes could not be measured for the negative-parity transitions due to the limited statistical accuracy of the RDM experiment.

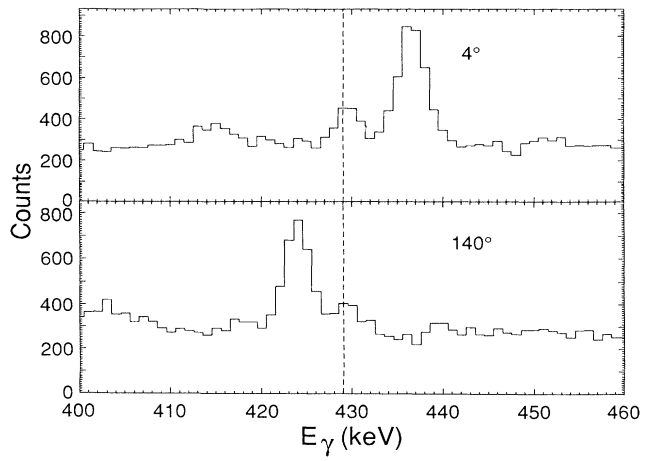

FIG. 6. Forward- and backward-angle coincidence line shapes for the 429.2 keV transition. The dashed line indicates the position of the unshifted peak.

V. DISCUSSION

The level scheme of ^{74}Br shows what appear to be two rotational bands. Their collective nature is confirmed by the electric quadrupole transitions within these bands which are enhanced by factors of 50 to 100 over single-particle values. A cranking-model analysis is appropriate to further investigate the rational properties of ^{74}Br and to compare them with neighboring nuclei.

A. Cranking model analysis

The kinematic ($J^{(1)}$) and dynamic ($J^{(2)}$) moments of inertia for the yrast band in ^{74}Br are shown in Fig. 7, along with those of neighboring nuclei. The $J^{(1)}$ values for ^{74}Br fall rapidly to about $22\hbar^2$/MeV at $\hbar\omega \approx$ 0.4 MeV and remain steady above that rotational frequency. The irregularities in level spacing at low spin which give rise to the high values of $J^{(1)}$ below 0.4 MeV have been attributed[7] to influence from various members of the $\pi g_{9/2} \otimes \nu g_{9/2}$ multiplet of states. Further evidence supporting this conclusion from the signature splitting will be presented later in this section. For the higher-spin states beyond this influence, the kinematic moments of inertia are as constant as any in the f-p-g shell. This constancy and the convergence of kinematic and dynamic moments of inertia show that ^{74}Br behaves as a good rotor at higher frequencies.

A companion study[6] of the yrast band of ^{76}Br which is based on a 4^+ state[19] shows a very similar behavior, providing additional justification for the spin assignments in ^{74}Br. In contrast, significant differences are seen in the low-spin behavior of neighboring odd-A and even-even nuclei. For example, $J^{(1)}$ remains[21] constant down to relatively low spins in the $g_{9/2}$ band in ^{73}Br, supporting the interpretation of multiplet influences on ^{74}Br. The graph of $J^{(1)}$ for the yrast band[22] in ^{74}Se in Fig. 7 is almost the mirror image of that of ^{74}Br. It rises from very low values at low spin to saturate at the common value of about $22\hbar^2$/MeV.

Both the differences in the kinematic moments of inertia at low spin and their similarities at high spin are somewhat systematic. For example, $J^{(1)}$ for ^{84}Zr (Ref. 23) also rises continuously from rather low values to saturate at $25\hbar^2$/MeV, a slightly higher value attributable to the higher mass. Shape coexistence[22,24] is known to affect the lowest levels in ^{74}Se, but it is not clear that this can explain the slow rise in $J^{(1)}$ over so many states or the similar behavior in heavier nuclei such as ^{84}Zr. Quasiparticle alignment may play a key role in the differences in $J^{(1)}$ at low spin since the effect seems to be correlated with the number of unpaired quasiparticles in the lowest configuration: 0 (^{74}Se), 1 (^{73}Br), 2 (^{74,76}Br).

There are no sharp excursions in the dynamical moments of inertia in ^{74,76}Br, unlike ^{73}Se (Ref. 25). This is consistent with the fact that the unpaired neutron and proton are expected to block the lowest band crossings.

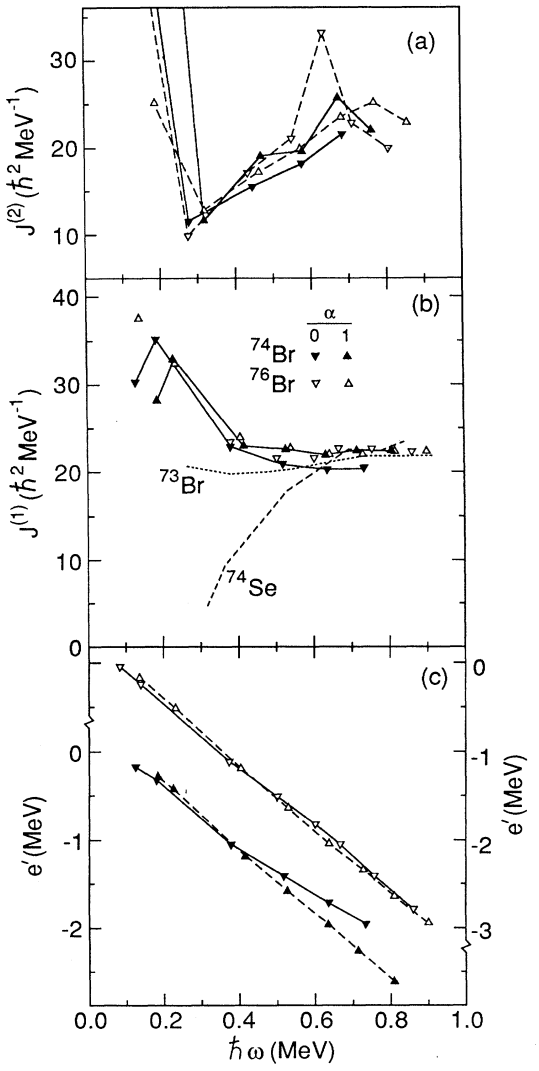

FIG. 7. (a) The dynamic moments of inertia $J^{(2)}$ for the yrast bands of ^{74,76}Br as a function of rotational frequency. The points for the lowest frequencies are off scale due to the expanded ordinate. (b) The kinematic moments of inertia $J^{(1)}$ for the yrast bands of ^{73,74,76}Br and ^{74}Se. The same symbols are used for ^{74,76}Br as in (a) but lines are not drawn connecting ^{76}Br points to reduce clutter. The two lowest ω ^{76}Br points with signature α=0 are off scale at about $45\hbar^2$/MeV. To further simplify the figure, the graphs for ^{73}Br and ^{74}Se are shown as lines without symbols. (c) Experimental Routhians (e') for ^{74,76}Br. Note that the right-hand ordinate scale applies to ^{76}Br and the left one to ^{74}Br. The Harris parameters used are $J_0 = 4\hbar^2$/MeV and $J_1 = 6\hbar^4$/MeV^3.

There is some evidence of a crossing with strong interaction in the α=1 signature of ^{74}Br at $\hbar\omega \approx 0.67$ MeV, but not in the α=0 signature within the frequency range that has been observed. Somewhat more distinct peaks in $J^{(2)}$ can be seen in ^{76}Br although the effects are still small and signature dependent.

The signature splitting in the yrast bands of ^{74,76}Br can be inferred from the experimental Routhians shown in Fig. 7(c). A standard Harris parametrization has been used for the rotational energy which was subtracted. We have used a set of Harris parameters ($J_0 = 14\hbar^2$/MeV

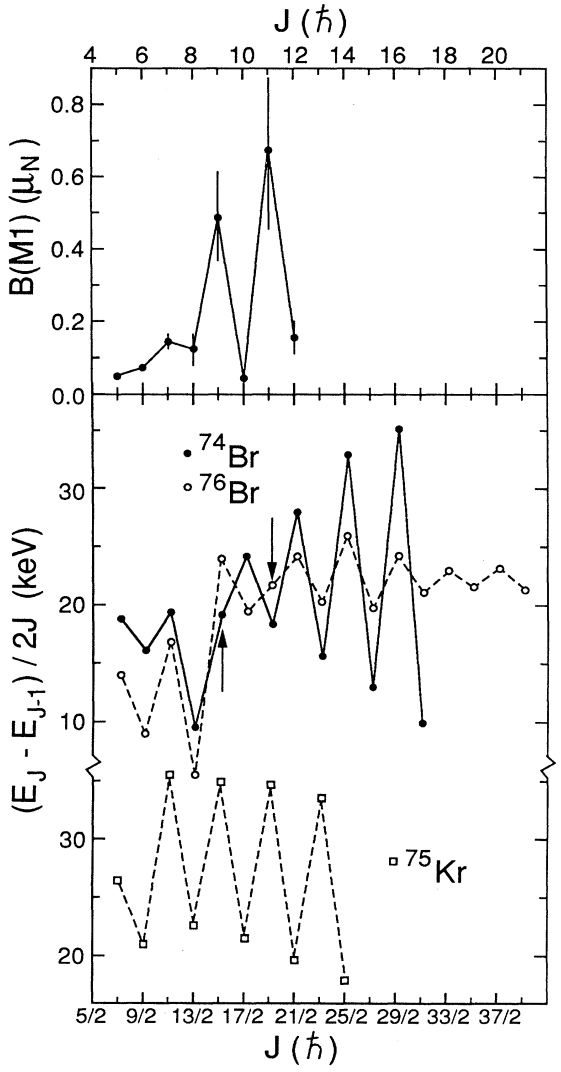

FIG. 8. Graphs of the quantity $(E_J - E_{J-1})/2J(=\hbar^2/2\theta)$ as a function of J for the yrast bands in ^{74,76}Br and ^{75}Kr. The arrows mark the points where the phase of the alternating pattern reverses. The $B(M1)$ strengths for the yrast band in ^{74}Br are also shown in the top part of the figure. Note that the lifetime of the 9^+ state was inferred from systematics as discussed in the text.

and $J_1 = 6\hbar^4/\text{MeV}^2$) which were determined[26] for ^{75}Kr, but the results discussed below are not sensitive to these values. At higher spins the signature splitting in ^{74}Br is large and increases with frequency, whereas that of ^{76}Br is significantly smaller and decreases with frequency. In the low-spin region the two isotopes exhibit similar signature splitting.

What is perhaps most interesting in Fig. 7(c) is that the sign of the signature splitting reverses at about $\hbar\omega =$ 0.4 MeV in both nuclei. The α=1 Routhians lie higher in energy below this frequency and lower above it.

The change in signature splitting can be seen more clearly (and independent of the Harris parametrization) by graphing the quantity $(E_J - E_{J-1})/2J$, as shown in Fig. 8. This quantity would have a constant value of $\hbar^2/2\theta$ for a perfect rotor and an alternating pattern in the presence of signature splitting. The variations discussed above in the magnitude of signature splitting as a function of frequency for ^{74,76}Br can be seen even more clearly in Fig. 8. The change in the sign of the signature splitting shows up here as a reversal of phase in the alternating pattern. These points of phase change ($9\hbar$ for ^{74}Br and $11\hbar$ for ^{76}Br) are indicated by arrows in Fig. 8. A graph of the same quantity for the yrast band of ^{75}Kr (Refs. 26 and 27) is shown in Fig. 8 for comparison. A similar large alternating pattern of signature splitting can be seen, but there is no change of phase. Somewhat arbitrarily the ^{75}Kr bandhead spin of $\frac{5}{2}$ was aligned in this figure with the bandhead spin of 4 for ^{74,76}Br. An alignment with odd Br spin would have placed the ^{75}Kr curve in phase with the high-spin Br curves rather than the low-spin region.

García Bermúdez *et al.*[5] have discussed the reversal of signature splitting in ^{74}Br. At that time their data extended just beyond the reversal and ^{76}Br was not known up to the reversal. Later Döring *et al.*[28] and Winchell *et al.*[29] observed the reversal in ^{76}Br. Prior to this, Kreiner and Mariscotti[4] predicted a reversal in ^{76}Br above $9\hbar$ based upon calculations in a two noninteracting quasiparticles plus rotor model. The significance of spin 9 is that it represents the highest value obtainable from the intrinsic motion of two $g_{9/2}$ particles in an odd-odd nucleus. Below it in the calculation the yrast states are based on a combination of collective rotation and realignment of the intrinsic spins. Above $9\hbar$ the band involves rotation of a system with two fully aligned quasiparticles. This change in structure leads to the reversal in signature splitting and to the differences in the kinematic moments of inertia.

Hamamoto[30] has also shown that a similar reversal in signature splitting in ^{156}Tb and ^{160}Ho can be accounted for in a two-quasiparticle-plus-rotor framework. The change also occurs near $j_p + j_n$, although the particles lie in different orbitals in this case. Kreiner and Mariscotti[31] have identified a change of phase in ^{108}In and discussed the general conditions for its occurrence. The reversal of signature splitting also occurs in some odd-A nuclei at the first band crossing, but it is not clear how similar this is to the odd-odd case. Ikeda and Shimano[32] have accounted for the reversal in $\pi h_{11/2}$ bands in terms of γ vibration.

The kinematic and dynamic moments of inertia for the K^π=(3$^-$) band in ^{74}Br are shown in Fig. 9. As in the positive-parity band, the kinematic moments decrease to a relatively constant value of about $23\hbar^2/\text{MeV}$. The dynamic moments show no large excursions, although there are weak peaks in the frequency range 0.4 to 0.5 MeV which may indicate a band crossing with a large interaction.

A plot of energy differences in the (3$^-$) band is shown in Fig. 10 for comparison with those in the yrast band. The alternations stay in phase throughout the spin region measured, except for the $J = 4$ point. The signature splitting decreases to nearly zero at $J = 10$ and then increases again, but there is no phase change.

B. Transition strengths and deformation

The adopted lifetimes from Table II were used to determine the $E2$ transition strengths $B(E2)$ for the $\Delta J = 2$ decays. The transition quadrupole moments Q_t were calculated from these strengths using the rotational model. Quadrupole deformations β_2 were, in turn, inferred from the moments assuming axial symmetry to get some idea of the shapes involved. These values are listed in Table III.

Some information can also be inferred about the $\Delta J =$ 1 transition strengths using branching ratios determined from the intensities in Table I. There is also angular dis-

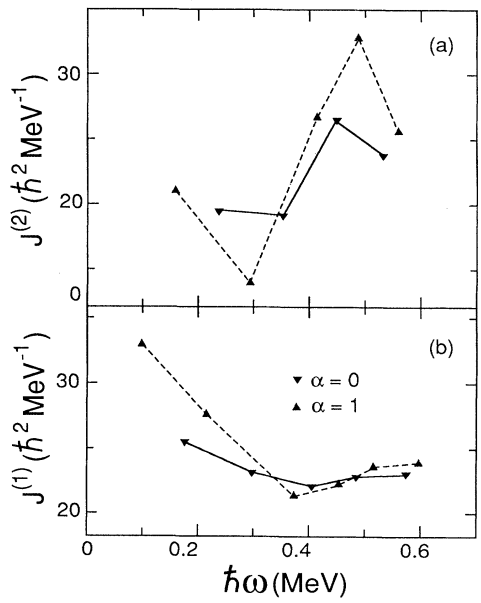

FIG. 9. Graphs of the (a) dynamic ($J^{(2)}$) and (b) kinematic ($J^{(1)}$) moments of inertia for the $K^\pi = (3^-)$ band in ^{74}Br.

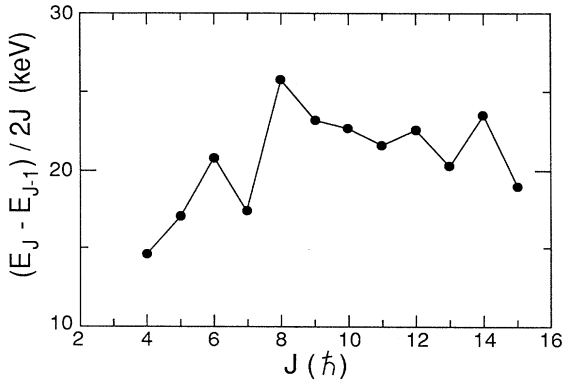

FIG. 10. A graph of $(E_J - E_{J-1})/2J$ for the $K^\pi = (3^-)$ band in ^{74}Br.

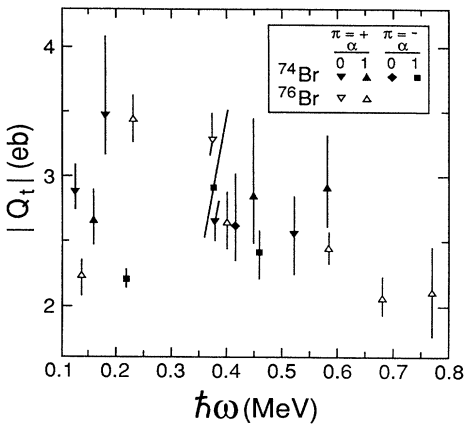

FIG. 11. Transition quadrupole moments $|Q_t|$ inferred from the mean lifetimes measured in ^{74}Br and ^{76}Br (Ref. 6).

tribution data available[5] in the form of Legendre polynomial coefficients. Mixing ratios were determined from the coefficients and used to calculate $B(M1)$ and $B(E2)$ transitions strengths. These are shown in Table IV. In those cases where the lifetime and branching ratio are known, but information is not available on the mixing ratio, it is still possible to reliably estimate the $M1$ but not the $E2$ strength. For these cases we have assumed a mixing ratio δ of 0.2, which is consistent with the measured values, since $B(M1)$ is rather insensitive to δ as long as it is small. No $B(E2)$ values are listed for these cases since they scale with δ^2.

As mentioned earlier most of the quadrupole transition strengths lie in the range of 50 to 100 single-particle units, indicating considerable collective enhancement. The quadrupole deformations (assuming axial symmetry) in the yrast band are relatively constant at $\beta_2 \approx 0.37$ indicating that ^{74}Br is very strongly deformed. Those in the negative-parity band are just a little lower, averaging $\beta_2 \approx 0.34$.

The transition quadrupole moments Q_t are shown in Fig. 11. They are also relatively constant with an average value of 2.9 e b in the yrast band and 2.5 e b in the negative-parity band. The similarity of Q_t values between low- and high-spin states suggests that mixing of other members of the $\pi g_{9/2} \otimes \nu g_{9/2}$ multiplet affects the energies of the low-spin states more than their transition probabilities.

The Q_t values[6] for the yrast band of ^{76}Br are also shown in Fig. 11 for comparison. The magnitudes are rather similar to those in ^{74}Br, implying a rather similar

TABLE III. Shown are the lifetimes, branching ratios, $E2$ transition strengths, transition quadrupole moments, and axial deformations for the $\Delta J = 2$ transitions in ^{74}Br.

I^π	τ (ps)	B.R. (%)	$B(E2)$ (W.u.)[a]	Q_T (e b)	β_2[b]
$6^{(+)}$	68.(8)	36(1)	28^{4}_{3}	2.9^{2}_{2}	0.38
$7^{(+)}$	13.(2)	33(1)	50^{16}_{9}	2.8^{3}_{2}	0.36
$8^{(+)}$	23.(7)	82(1)	108^{10}_{9}	3.5^{7}_{4}	0.45
$10^{(+)}$	1.19(14)	93(1)	86^{11}_{9}	2.6^{2}_{1}	0.35
$11^{(+)}$	0.45(15)	63(1)	108^{54}_{27}	2.8^{6}_{4}	0.37
$12^{(+)}$	0.23(6)	79(3)	92^{32}_{19}	2.5^{4}_{3}	0.34
$13^{(+)}$	0.21(5)	100(1)	126^{39}_{24}	2.9^{4}_{3}	0.38
(14^+)	<0.19	100(1)	>56	>1.9	>0.26
(15^+)	<0.24	100(1)	>47	>1.7	>0.23
(7^-)	17.(1)	57(1)	52^{3}_{3}	2.2^{1}_{1}	0.30
(9^-)	0.60(20)	61(2)	117^{58}_{29}	2.9^{7}_{4}	0.38
(10^-)	0.70(17)	78(3)	101^{32}_{20}	2.6^{4}_{3}	0.35
(11^-)	0.54(12)	75(1)	89^{25}_{16}	2.4^{3}_{2}	0.32
(12^-)	<0.50	100(1)	>82	>2.2	>0.30
(13^-)	<0.53	100(1)	>60	>1.9	>0.26

[a] 1 W.u. = 18.4 e^2 fm^4.
[b] Assuming axial symmetry.

TABLE IV. $M1$ and $E2$ transition strengths for $\Delta J = 1$ transitions in ^{74}Br. The mixing ratios δ were determined from the angular distribution data in Ref. 5. For those transitions whose angular distributions are not known a value of δ=0.2 was assumed.

J^π	E_γ (keV)	δ	$B(E2)$ (W.u.)	$B(M1)$ (μ_N^2)
$5^{(+)}$	188	0.2[a]		0.05(1)
$6^{(+)}$	195	0.23	74	0.07(1)
$7^{(+)}$	273	0.25	88	0.14(2)
$8^{(+)}$	156	0.12	53	0.12(4)
$9^{(+)}$	348	0.2[a]		0.48(12)[b]
$10^{(+)}$	486	0.2[a]		0.04(1)
$11^{(+)}$	408	0.16	80	0.67(22)
$12^{(+)}$	698	0.2[a]		0.15(4)
(9^-)	415	0.2[a]		0.50(17)
(10^-)	452	0.2[a]		0.19(5)
(11^-)	476	0.2[a]		0.24(5)

[a] Assumed value, see text.
[b] Assumed τ = 2.3(5) ps so that Q_t=2.85(40) e b for the $9^{(+)} \rightarrow 7^{(+)}$ transition.

deformation. There may be some difference between the apparent decreasing trend in Q_t for ^{76}Br and the more constant value for ^{74}Br. However, lifetimes have not been measured as far up the band in ^{74}Br and the uncertainties may not permit so detailed a comparison.

The unknown lifetime for the 9^+ state is important in determining the pattern of $B(M1)$ strengths since no $\Delta J = 1$ transitions have been observed from states above the 12^+ level. Since the $\Delta J = 2$ transition quadrupole moments are relatively constant above and below the 9^+ state, we have assumed that Q_t for the $9^+ \rightarrow 7^+$ transition is the average value of 2.85 $\pm$ 0.40 e b to estimate the lifetime of the 9^+ state (2.3 $\pm$ 0.5 ps) and hence the $9^+ \rightarrow 8^+$ $B(M1)$ strength [(0.48 $\pm$ 0.12)μ_N^2]. The magnetic transition strengths are listed in Table IV and graphed in the upper part of Fig. 8. An alternating pattern can be seen, especially for the higher spin states. The pattern is consistent with the calculations[30] of Hamamoto for ^{156}Tb which show $B(M1)$ strengths alternating out of phase with the energy differences.

C. Hartree-Fock-Bogolyubov cranking calculations

Calculations were performed[9] for ^{74}Br using the Woods-Saxon cranking model of Ref. 33. The pairing force was assumed to be of the monopole type, and the rotation was treated by means of the cranking approximation. The procedure used here has been described in Refs. 2 and 34.

Some calculated total Routhian surfaces (TRS) in the (β_2,γ) plane are shown in Fig. 12. At each (β_2,γ) grid point the total Routhian was minimized with respect to the hexadecupole deformation β_4. The result for the aA configuration at a rotational frequency of $\hbar\omega$ = 0.3 MeV is typical for the yrast band up to 0.8 MeV. The quasiparticle labeling scheme is defined in Ref. 35. Lower (upper) case letters are used for the proton (neutron) configuration. For example, a (A) represents the lowest unique parity orbital, which is $g_{9/2}$ for protons (neutrons). The well-deformed nearly prolate minimum lies at (β_2,γ) = (0.33,$-4°$). A minimum in the TRS remains near this point over a wide frequency range and is the absolute minimum in the range 0.1 MeV $\leq \hbar\omega \leq$0.7 MeV. The deformation β_2 at the minimum decreases very slowly with increasing frequency from 0.35 to 0.30. The deformation inferred from the lifetime measurements (0.37 average) is rather similar to the predicted values. The uncertainties are too large to confirm whether a decreasing trend in β_2 is observed in ^{74}Br, but there may be such evidence in ^{76}Br.

The TRS shown in Fig. 12 for the aE configuration ($\pi = -$, $\alpha = -\frac{1}{2}$ neutron) at $\hbar\omega$ = 0.3 MeV is typical of those predicted for the negative-parity band. The calculated deformation (β_2,γ) = (0.35,$-0.9°$) is very close to the measured value (0.34 average). Hence predicted and measured deformations are rather similar in both bands and the small differences lie within the uncertainties in the measurements and calculations.

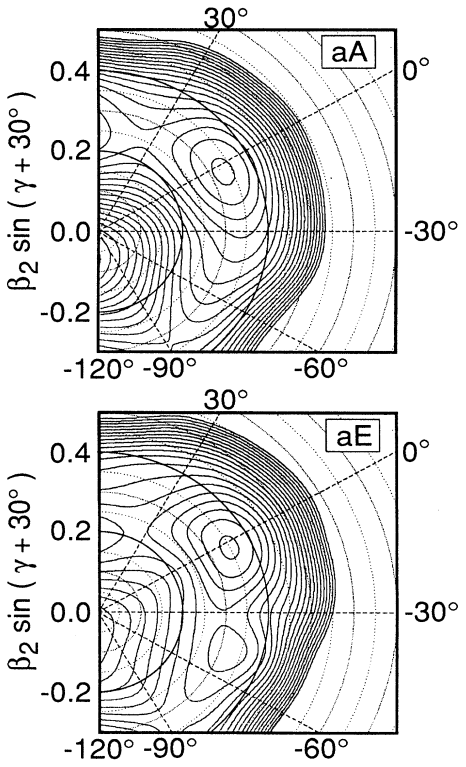

FIG. 12. Total Routhian surfaces (with pairing) in the (β_2,γ) polar coordinate plane for ^{74}Br at a rotational frequency of $\hbar\omega$ = 0.3 MeV. The letters in the boxes indicate the quasiparticle configurations as discussed in the text. The interval between contour lines is 0.25 MeV.

VI. SUMMARY

High-spin states in ^{74}Br were produced in two different heavy-ion fusion-evaporation reactions. Two rotational bands were extended up to tentative spins of (15^-) and (19^+). DCO ratios were used in assigning spins, and mean lifetimes were measured using both the Doppler-shift attenuation and recoil-distance methods.

Determination of the bandhead spins and parities in this odd-odd nucleus is problematical because of the β-decaying isomer. It appears that both bands populated strongly in the heavy-ion reactions are built upon or decay to the spin-4 isomer. Even the parity of this isomer is not firmly established, although π=+ is strongly suggested from comparisons with ^{76}Br and other nearby nuclei.

The $4^{(+)}$ band in ^{74}Br is very similar to that in ^{76}Br. Fast electric quadrupole transitions in both bands of ^{74}Br imply strongly deformed shapes with $\beta_2 = 0.37$ for the $K^\pi = 4^{(+)}$ band and 0.34 for the $K^\pi = (3^-)$ band. At higher spins both bands behave as good rotors with a rather constant kinematic moment of inertia ($J^{(1)} \approx 22\hbar^2$/MeV) which is relatively close to the dynamical moment of inertia. The energies of the lower-spin states are less regular, suggesting admixtures of various members of the $\pi g_{9/2} \otimes \nu g_{9/2}$ multiplet with the collective rotational states in the yrast band. The structural difference between the low and high spin states of the yrast bands of ^{74}Br and ^{76}Br shows up rather clearly as a reversal in the signature splitting around $\hbar\omega \approx 0.4$ MeV. The experimental Routhians for the two signatures (α=0 and 1) cross at this frequency, and the phase of the alternating pattern of energy differences reverses around spin 10.

The magnetic transition strengths show an alternating pattern which is related to the signature splitting. The transition quadrupole moments Q_t are rather similar in the yrast bands of ^{74}Br and ^{76}Br and in the negative parity band of ^{74}Br, indicating a similar degree of deformation in all three bands. There is some evidence for a decreasing trend in the Q_t values, especially in ^{76}Br.

Hartree-Fock-Bogolyubov cranking calculations predict a rather stable, nearly prolate shape for both bands in ^{74}Br. The predicted quadrupole deformations of $\beta_2 = 0.33$ (0.35) for the positive- (negative-) parity bands are close to the values deduced from the experimentally measured lifetimes.

ACKNOWLEDGMENTS

We wish to thank W. Nazarewicz for informative discussions and for providing the Hartree-Fock-Bogolyubov cranking calculations. This work was supported in part by the National Science Foundation. Two of us (S.G.B. and F.E.D.) acknowledge support through the Louisiana Board of Regents Experimental Program to Stimulate Cooperative Research (EPSCoR) Grant No. NSF/LaSER (1989)-RFAP-05.

[1] S. E. Arnell, C. Ekström, L. P. Ekström, A. Nilsson, I. Ragnarsson, P. J. Smith, and E. Wallander, J. Phys. G **9**, 1217 (1983).
[2] E. F. Moore, P. D. Cottle, C. J. Gross, D. M. Headly, U. J. Hüttmeier, S. L. Tabor, and W. Nazarewicz, Phys. Rev. C **38**, 696 (1988).
[3] G. C. Hicks, C. J. Gross, U. J. Hüttmeier, Xi- Ting Lu, G. Neuschaefer, and S. L. Tabor, Phys. Rev. C **30**, 549 (1984).
[4] A. J. Kreiner and M. A. J. Mariscotti, Phys. Rev. Lett. **43**, 1150 (1979).
[5] G. García Bermúdez, A. Filevich, A. J. Kreiner, M. A. J. Mariscotti, C. Baktash, E. der Mateosian, and P. Thieberger, Phys. Rev. C **23**, 2024 (1981).
[6] S. G. Buccino, F. E. Durham, J. W. Holcomb, T. D. Johnson, P. D. Cottle, and S. L. Tabor, Phys. Rev. C **41**, 2056 (1990).
[7] G. Winter, J. Döring, W. D. Fromm, L. Funke, P. Kemnitz, and E. Will, Z. Phys. A **309**, 243 (1982).
[8] W. Neumann, L. Cleeman, J. Eberth, J. Heck, G. S. Li, M. Nolte, and J. Roth, in *Proceedings of the Conference on High Angular Momentum Properties of Nuclei*, Oak Ridge, Tennessee, 1982, edited by Noah R. Johnson (Oak Ridge National Laboratory, Oak Ridge, 1982), Vol. 1, p. 66.
[9] W. Nazarewicz, private communication.
[10] S. L. Tabor, Nucl. Instrum. Methods A **265**, 495 (1988).
[11] K. S. Krane, R. M. Steffen, and R. M. Wheeler, Nucl. Data Tables **11**, 354 (1973).
[12] A. Coban, J. Phys. A **7**, 1705 (1974.
[13] H. Schmeing, J. C. Hardy, R. L. Graham, and J. S. Geiger, Nucl. Phys. **A242**, 232 (1975).
[14] H. Schmeing, R. L. Graham, J. C. Hardy, and J. J. Geiger, Nucl. Phys. **A233**, 63 (1974).
[15] A. Coban, J. C. Lisle, G. Murray, and J. C. Willmott, Part. Nuclei **4**, 108 (1972).
[16] D. H. Lueders, J. M. Daley, S. G. Buccino, F. E. Durham, C. E. Hollandsworth, W. P. Bucher, and H. D. Jones, Phys. Rev. C **11**, 1470 (1975).
[17] C. Ekstrom and L. Robertson, Phys. Scr. **22**, 344 (1980).
[18] S. Raman and N. B. Gove, Phys. Rev. C **7**, 1995 (1973).
[19] A. J. Kreiner, G. García Bermúdez, M. A. J. Mariscotti, and P. Thieberger, Phys. Lett. **83B**, 31 (1979).
[20] L. C. Northcliffe and R. F. Schilling, Nucl. Data Sec. A **7**, 233 (1970).
[21] J. Heese, N. Martin, C. J. Gross, W. Fieber, K. P. Lieb, A. Kuhnert, K. H. Maier, and X. Sun, Phys. Rev. C **41**, 1553 (1990).
[22] P. D. Cottle, J. W. Holcomb, T. D. Johnson, K. A. Stuckey, S. L. Tabor, P. C. Womble, S. G. Buccino, and F. E. Durham (unpublished).
[23] H. G. Price, C. J. Lister, B. J. Varley, W. Gelletly, and J. W. Olness, Phys. Rev. Lett. **51**, 1842 (1983).
[24] R. B. Piercey, A. V. Ramayya, R. M. Ronningen, J. H. Hamilton, V. Maruhn-Rezwani, R. L. Robinson, and H. J. Kim, Phys. Rev. C **19**, 1344 (1979).
[25] Li Guangsheng, L. Cleemann, J. Eberth, T. Heck, W. Neumann, M. Nolte, and J. Roth, Chin. J. Nucl. Phys. **5**, 225 (1983).
[26] A. A. Chisti, W. Gelletly, C. J. Lister, J. H. McNeill, B. J. Varley, D. J. G. Love, and O. Skeppstedt, Nucl. Phys. **A501**, 568 (1989).

[27]D. F. Winchell, M. S. Kaplan, J. X. Saladin, H. Takai, J. J. Kolata, and J. Dudek, Phys. Rev. C **40**, 2672 (1989).
[28]J. Döring, G. Winter, L. Funke, P. Kemnitz, and E. Will, Z. Phys. A **305**, 365 (1982).
[29]D. F. Winchell, J. X. Saladin, M. S. Kaplan, and H. Takai, Phys. Rev. C **41**, 1264 (1990).
[30]Ikuko Hamamoto, Phys. Lett. B **235**, 221 (1990).
[31]A. J. Kreiner and M. A. J. Mariscotti, J. Phys. G **6**, L13 (1980).
[32]Akitsu Ikeda and Takafumi Shimano, Phys. Rev. C **42**, 149 (1990).
[33]W. Nazarewicz, J. Dudek, R. Bengtsson, T. Bengtsson, and I. Ragnarsson, Nucl. Phys. **A435**, 397 (1985).
[34]U. J. Hüttmeier, C. J. Gross, D. M. Headly, E. F. Moore, S. L. Tabor, T. M. Cornier, P. M. Swertka, and W. Nazarewicz, Phys. Rev. C **37**, 118 (1988).
[35]R. Wyss, F. Lidén, J. Nyberg, A. Johnson, D. J. G. Love, A. H. Nelson, D. W. Banes, J. Simpson, A. Kirwan, and R. Bengtsson, Nucl. Phys. **A503**, 244 (1989).